Rev. Roum. Sci. Techn.– Électrotechn. et Énerg.
Vol. **67**, *2*, pp. 99–104, Bucarest, 2022

STABILITY AND ACCURACY IMPROVEMENT OF MOTOR CURRENT ESTIMATOR IN LOW-SPEED OPERATING BASED ON SLIDING MODE TAKAGI-SUGENO ALGORITHM

AIMAD AHRICHE[1], IDIR ABDELHAKIM[1], MOHAMED ZINLABIDINE DOGHMANE[1], MADJID KIDOUCHE[1], SAAD MEKHILEF[2]

Keywords: Sliding mode observer; Fuzzy logic controller; Volt per Hertz (*v/f*) control; Lyapunov's theorem.

This paper is devoted to presenting a new mathematical development and hardware implementation of an accurate and stable technique for the current estimation-based sliding mode observer in high-performance speed-sensorless ac-drive. The proposed algorithm is built by using induction motor (IM) flux equations in two referential frames to enhance the robustness of the observer. Indeed, all equations are given in both stator-flux and rotor-flux rotating frames. On the other hand, to eliminate the necessity of rotor-speed adaptation, a fully speed-sensorless scheme is adopted. Furthermore, to minimize chattering and improve accuracy, a new fuzzy sliding surface is introduced instead of the conventional correction vector. The observer stability is guaranteed by means of Lyapunov's second method. The feasibility and the effectiveness of the proposed algorithm are verified by using a hardware setup based on the DS1104 controller board. Experimental results are shown and discussed.

1. INTRODUCTION

In recent years, state observers and/or parameter estimators have been widely investigated and developed in machine drive. This is mainly because of their huge influence on the performance control part, especially for a sensorless drive [1–5]. Overall, a high-performance drive relies heavily on the measurement of the terminal quantities such as voltages, currents, and rotor speed. Hence, the use of accurate and reliable sensors is mandatory despite its high cost. However, in some cases, when the measurement is not available or undesired such as in a sensorless scheme, a high-performance drive can also be obtained by using state observers. Therefore, the features of the state observers and/or parameter estimators have taken an interesting place in the development of ac drives. Among observation techniques, we can cite the well-known sliding mode observer (SMO) which has imposed itself in the domain of ac drive. Their prominence returns to its advantages which include fast convergence, disturbances rejection, simple implementation, and robustness to model parameters influence, especially at very low speed and standstill conditions.

In nowadays, many researchers have put forward a lot of topologies and techniques of the sliding mode observer to improve their performance and dynamic [6–11]. In [6], three topologies of speed-sensorless SMO are presented and compared. Where the merits of the dual reference frame topology are appeared well than in the two other topologies, especially against the mutual inductance mismatch. A comparison between sliding mode observer and extended Kalman filter is performed in [7], whereas some developments of the SMO performance for permanent magnet synchronous motor (PMSM) drives are presented in [8–11]. A Class of Parabolic function-based surfaces is presented and discussed in [12–14], In [14], the authors present an experimental investigation of induction motor state estimation based on the combining of sliding mode and Lyapunov's second function principles. Moreover, a hyperbolic function with an adjustable slope is introduced in order to cover chattering effects. In [15], the fuzzy logic approach is introduced with sliding mode control.

In this paper, new mathematical development, and hardware implementation of fuzzy sliding mode observer (FSMO) is introduced. The proposed algorithm is built by using flux equations in a dual referential frame to enhance the robustness of the observer. The stator-flux equation is given in the stator-flux rotating frame, whereas the rotor-flux equation is expressed in the rotor-flux referential frame. On the other hand, to eliminate the necessity of the rotor-speed adaptation, a fully speed-sensorless scheme is adopted. Furthermore, to minimize chattering, a new fuzzy sliding surface is introduced instead of the conventional correction vector. The observer stability is guaranteed by means of Lyapunov's second method. The feasibility and the effectiveness of the proposed algorithm are verified by using a hardware setup based on the DS1104 controller board. Experimental results are shown and discussed.

2. THE PROPOSED SLIDING MODE OBSERVER

2.1. OBSERVER SYNTHESIS

The induction-motor flux-based model, in an arbitrary rotating reference frame denoted by (e), can be expressed as follow [16–18]

$$\frac{\mathrm{d}}{\mathrm{d}t}\underline{\lambda}_s^{(e)} = \frac{R_s}{\sigma L_s}\left(\frac{L_m}{L_r}\underline{\lambda}_r^{(e)} - \underline{\lambda}_s^{(e)}\right) - \mathrm{j}\omega_e \underline{\lambda}_s^{(e)} + \underline{u}_s^{(e)}, \tag{1}$$

$$\frac{\mathrm{d}}{\mathrm{d}t}\underline{\lambda}_r^{(e)} = \frac{R_r}{\sigma L_r}\left(\frac{L_m}{L_s}\underline{\lambda}_s^{(e)} - \underline{\lambda}_r^{(e)}\right) - \mathrm{j}(\omega_e - \omega_r)\underline{\lambda}_r^{(e)} \tag{2}$$

where, $\underline{\lambda}_s^{(e)}$ and $\underline{\lambda}_r^{(e)}$ are two vectors that represent the flux-linkage of both stator and rotor armatures respectively, ω_e is the angular speed of the arbitrary rotating reference frame and ω_r is the rotor angular speed. In addition, $\underline{u}_s^{(e)}$ represents the applied voltage vector and both of R_r, L_s, L_r, L_m and σ represent the IM-model parameters (given in the appendix).

The proposed scheme is built based on the following orientations:

[1]Laboratoire d'automatique appliquée, Faculté des hydrocarbures et de la chimie, Université de Boumerdes, Boumerdes, Algérie,
E-mail : a.ahriche@univ-boumerdes.dz

- equation (1) in stator-flux rotating reference-frame denoted by (*sf*)
- equation (2) in rotor-flux rotating reference-frame denoted by (*rf*)

$$\frac{\mathrm{d}}{\mathrm{d}t}\hat{\underline{\lambda}}_s^{(sf)} = \frac{R_s}{\sigma L_s}\left(\frac{L_m}{L_r}\hat{\underline{\lambda}}_r^{(sf)} - \hat{\underline{\lambda}}_s^{(sf)}\right) - \mathrm{j}\omega_{sf}\hat{\underline{\lambda}}_s^{(sf)} + \underline{u}_s^{(sf)} + \underline{k}_1^{(sf)}\underline{\mu}^{(sf)}, \tag{3}$$

$$\frac{\mathrm{d}}{\mathrm{d}t}\hat{\underline{\lambda}}_r^{(rf)} = \frac{R_r}{\sigma L_r}\left(\frac{L_m}{L_s}\hat{\underline{\lambda}}_s^{(rf)} - \hat{\underline{\lambda}}_r^{(rf)}\right) - \mathrm{j}(\omega_{sf} - \omega_r)\hat{\underline{\lambda}}_r^{(rf)} + \underline{k}_2^{(rf)}\underline{\mu}^{(rf)}. \tag{4}$$

The subscript (^) denotes the estimated value of variables k_1 and k_2 are the observer gains and $\underline{\mu}$ is the correction vector.

In stator-flux reference-frame, only the direct component of the stator-flux vector is considered, $\lambda_s^{(sf)} = \lambda_{sd}^{(sf)}$, and $\lambda_{sq}^{(sf)} = 0$. Thus, the stator flux equation in (3) becomes

$$\frac{\mathrm{d}}{\mathrm{d}t}\hat{\underline{\lambda}}_{sd}^{(sf)} = \frac{R_s}{\sigma L_s}\left(\frac{L_m}{L_r}\hat{\underline{\lambda}}_{rd}^{(sf)} - \hat{\underline{\lambda}}_{sd}^{(sf)}\right) + \underline{u}_{sd}^{(sf)} + \underline{k}_{1d}^{(sf)}\underline{\mu}_d^{(sf)}. \tag{5}$$

Similarly, in the rotor-flux reference frame only the direct component of the rotor-flux vector is considered, and $\lambda_{rq}^{(rf)} = 0$, the rotor-flux eq. (4) becomes

$$\frac{\mathrm{d}}{\mathrm{d}t}\hat{\underline{\lambda}}_{rd}^{(rf)} = \frac{R_r}{\sigma L_r}\left(\frac{L_m}{L_r}\hat{\underline{\lambda}}_{sd}^{(rf)} - \hat{\underline{\lambda}}_{rd}^{(rf)}\right) + \underline{k}_2^{(rf)}\underline{\mu}_d^{(rf)}. \tag{6}$$

The correction mechanism is of fuzzy-sliding-mode type based on the error between the actual stator-current value and its estimated value. The main idea of this hybrid observer is the fuzzification, by using Takagi-Sugeno fuzzy controller, of the observer's discontinuous part to generate a reached part. Hence the following surface (s) is used as input in the stationary reference frame

$$\underline{s} = \underline{i}_s^{(s)} - \hat{\underline{i}}_s^{(s)}, \tag{7}$$

and

$$\hat{\underline{i}}_s^{(s)} = \frac{1}{\sigma L_s}\left(\frac{L_m}{L_r}\hat{\underline{\lambda}}_r^{(s)} - \hat{\underline{\lambda}}_s^{(s)}\right), \tag{8}$$

where the subscript (*s*) denotes the stationary reference frame.

The membership functions of the two variables (s and μ) are illustrated in Fig.1

The rules of the used fuzzy controller (FLC) are given by:

- **R1**: if *S* is **GN** then μ is **GP**
- **R2**: if *S* is **N** then μ is **P**
- **R3**: if *S* is **Z** then μ is **Z**
- **R4**: if *S* is **P** then μ is **N**
- **R5**: if *S* is **GP** then μ is **GN**

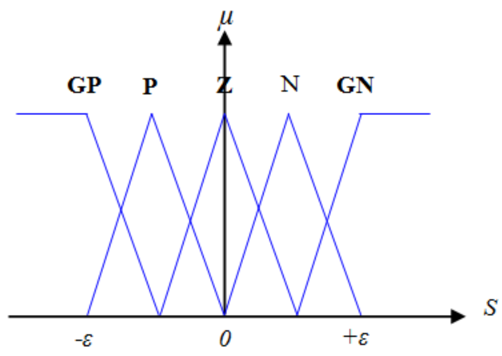

Fig. 1 – Membership functions of the used sliding surface.

The block scheme with inputs, state variables and estimated quantities is given in Fig. 2.

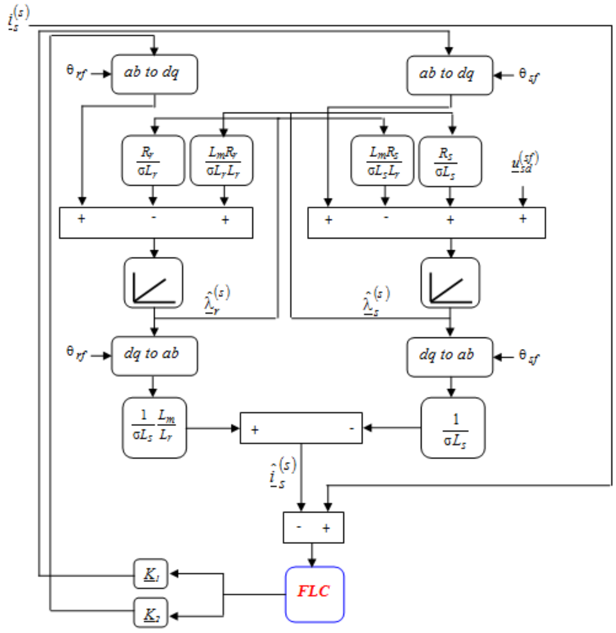

Fig. 2 – The proposed sliding mode observer-based state estimation.

2.2. STABILITY ANALYSIS

To satisfy the stability condition, the observer gain is confined based on direct Lyapunov's method. With the assumption that there is non-mismatch in the motor model parameters, the first derivative of the current error is

$$\frac{\mathrm{d}}{\mathrm{d}t}\underline{s} = \frac{1}{\sigma L_s}\left(\frac{L_m}{L_r}\frac{\mathrm{d}}{\mathrm{d}t}\left(\underline{\lambda}_r^{(s)} - \hat{\underline{\lambda}}_r^{(s)}\right) - \frac{\mathrm{d}}{\mathrm{d}t}\left(\underline{\lambda}_s^{(s)} - \hat{\underline{\lambda}}_s^{(s)}\right)\right). \tag{9}$$

Similarly, for the flux.

3. **EXPERIMENTAL RESULTS**

The implementation of the proposed algorithm is carried out by means of a high operating-speed Dsp1104 controller board. The whole studied system consists of a 3 kW squirrel-cage induction motor, which is used to drive the mechanical load (specifications and data are given in the appendix). The terminal voltage of the IM is generated through a three-phase pulse width modulation voltage source inverter with a switching frequency of 2.5 kHz. Both MATLAB and Control-Desk software are combined to manage the Dspace DS1104 board. The sampling frequency is set to 10 kHz.

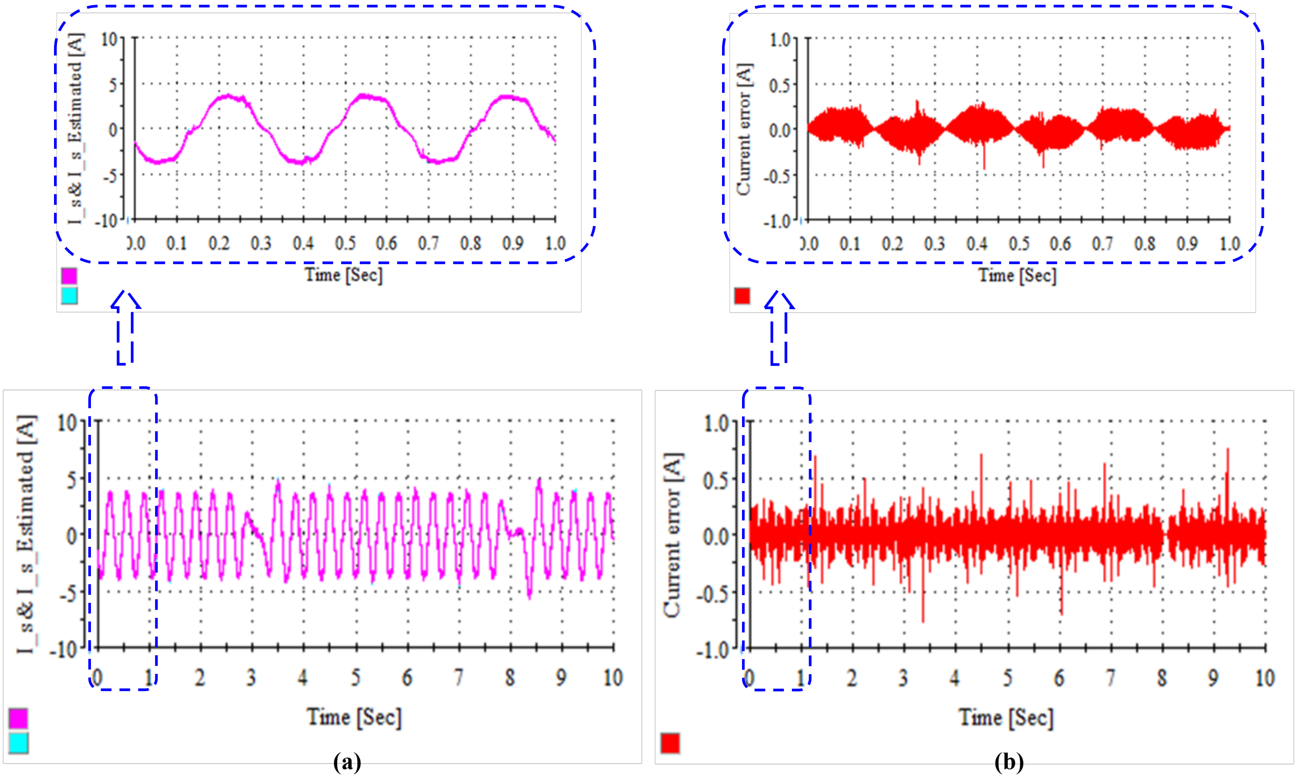

Fig 3 – Experimental results at the frequency of ± 3Hz with signum-function based SMO.
a) Estimated stator current *vs.* actual stator current. b) Error between estimated and actual currents.

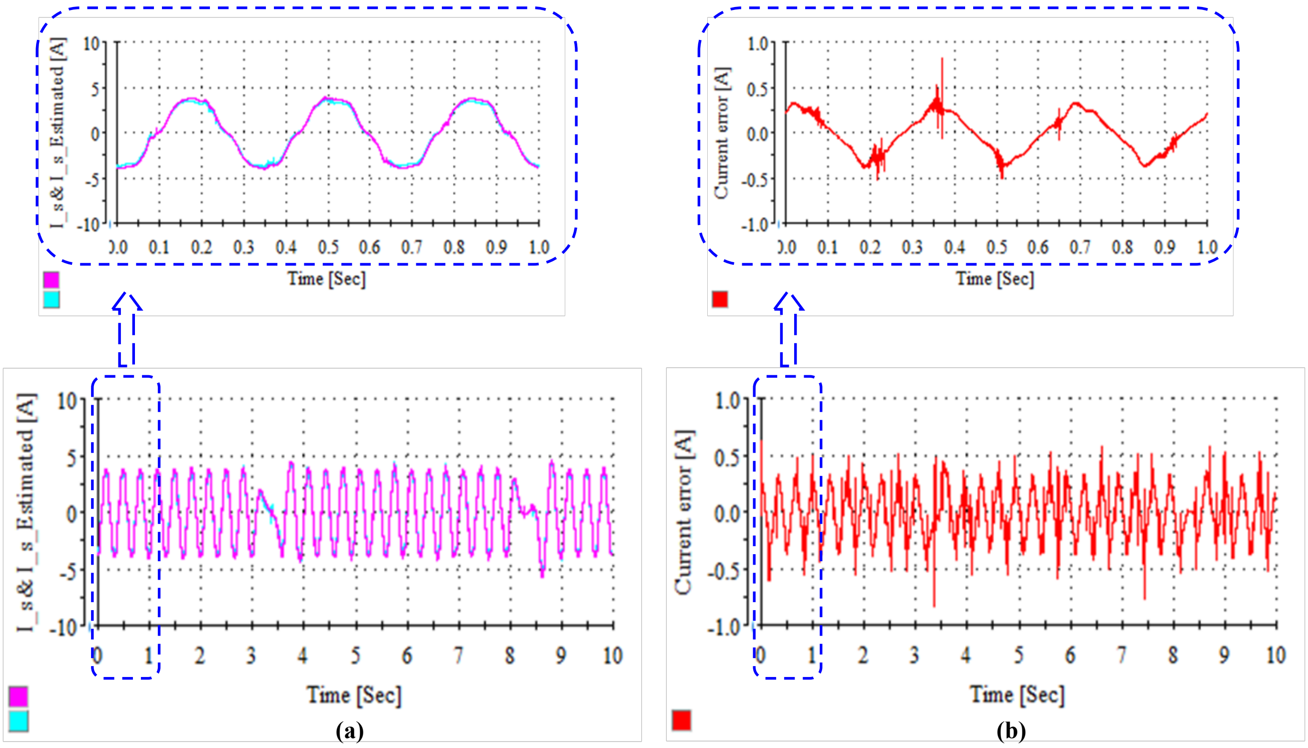

Fig 4 – Experimental results at the frequency of ± 3Hz with **saturation-function** based SMO.
a) Estimated stator current *vs.* actual stator current. b) Error between estimated and actual currents.

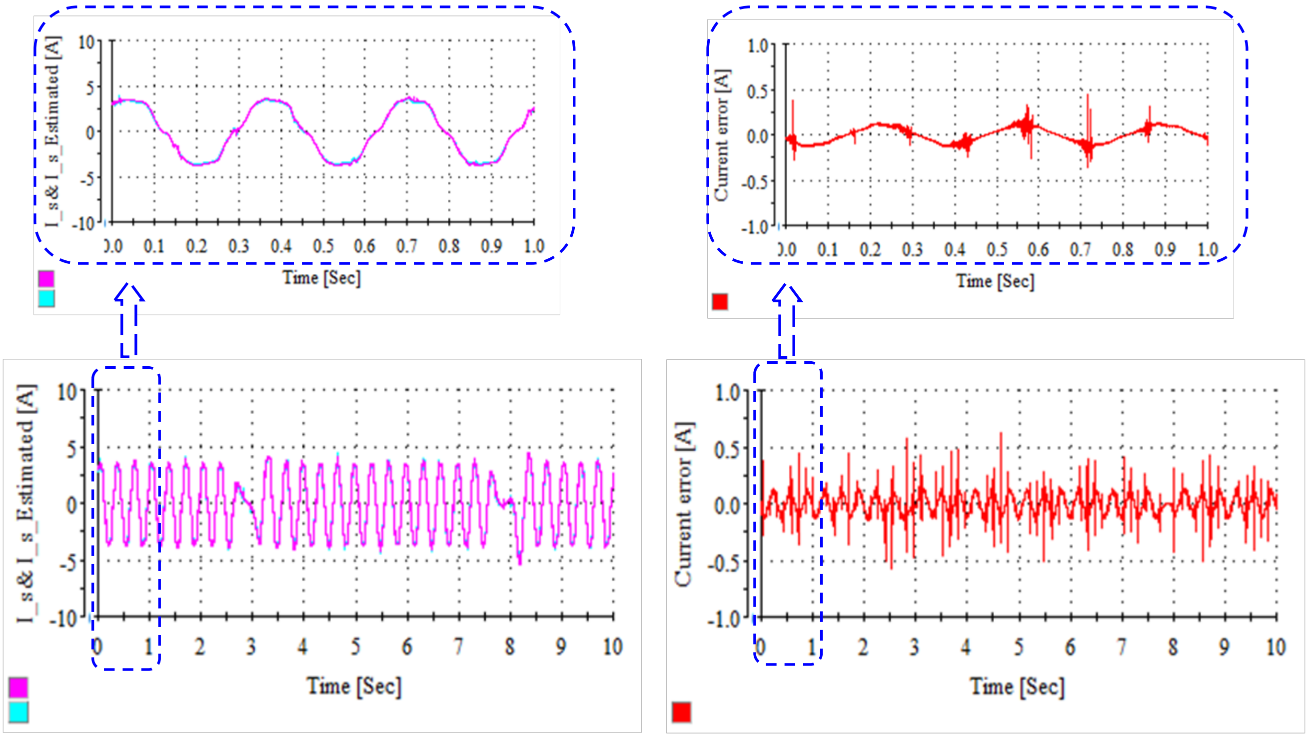

(a) **(b)**

Fig 5 – Experimental results at the frequency of ± 3Hz with Takagi-Sugeno FLC based SMO.
a) Estimated stator current *vs*. actual stator current. b) Error between estimated and actual currents.

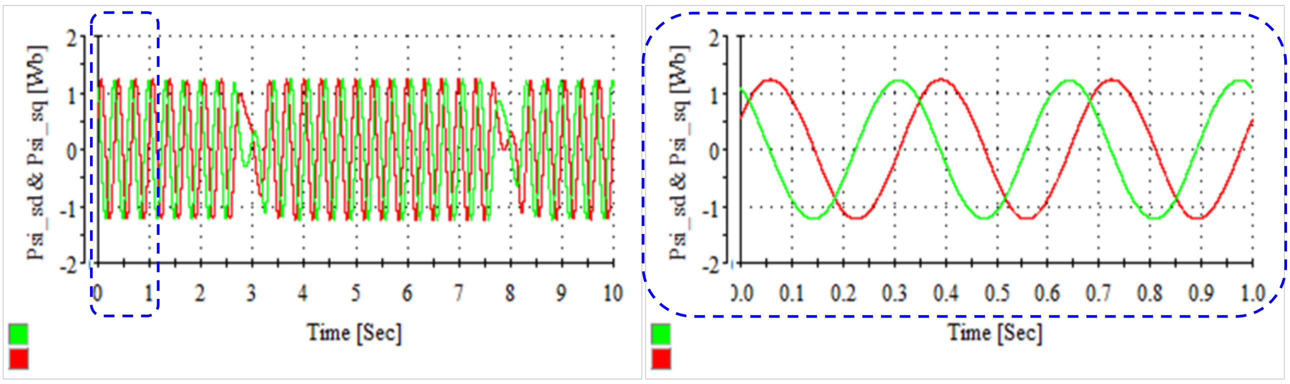

Fig 6 – Experimental results at the frequency of ± 3 Hz with Takagi-Sugeno FLC based SMO.

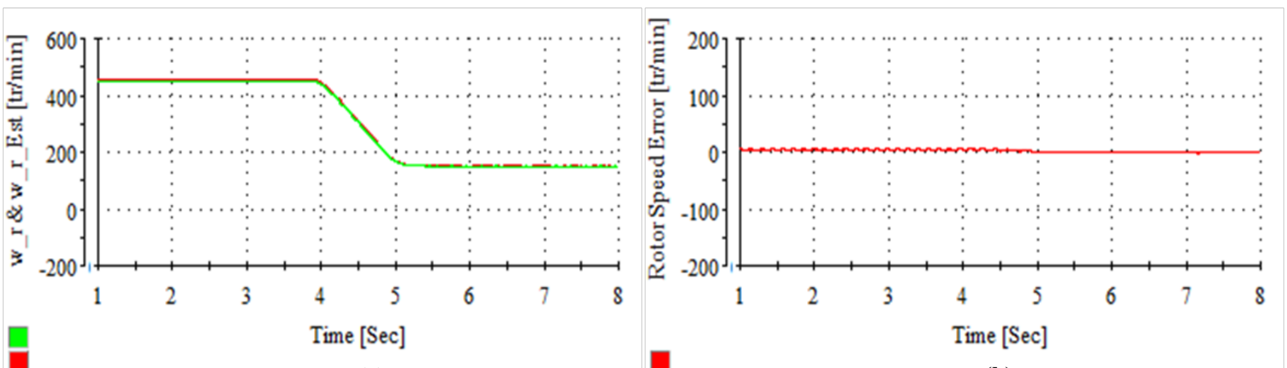

(a) **(b)**

Fig 7- Experimental results at the frequency of +15Hz and +5Hz with Takagi-Sugeno FLC based SMO.
a) Estimated rotor speed Vs actual speed. b) Error between estimated and real rotor speeds

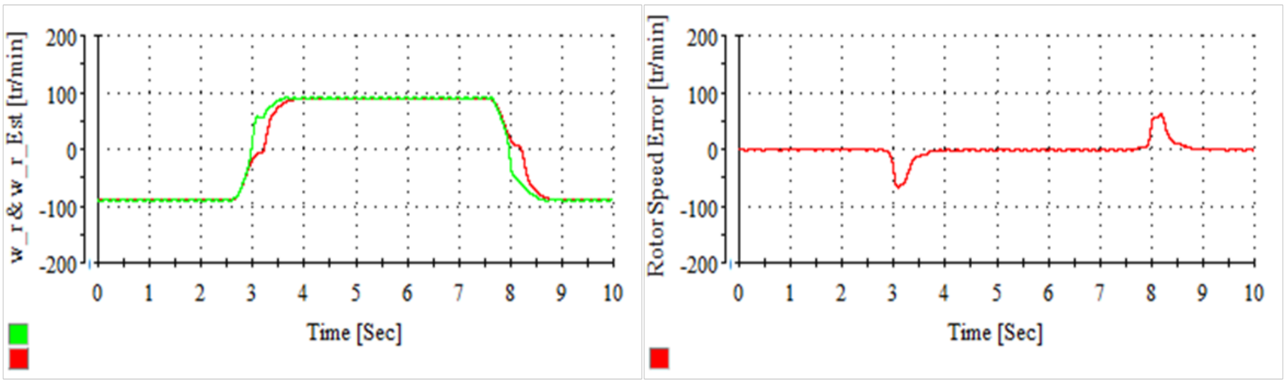

Fig 8. Experimental results at the frequencies of ±5 Hz by using a Takagi-Sugeno FLC based SMO.
a) Estimated rotor speed *vs*. actual speed. b) Error between estimated and real rotor speeds.

$$\frac{\mathrm{d}}{\mathrm{d}t}\left(\underline{\lambda}_s^{(sf)}-\hat{\underline{\lambda}}_s^{(sf)}\right)=\frac{R_sL_m}{\sigma L_sL_r}\left(\underline{\lambda}_r^{(sf)}-\hat{\underline{\lambda}}_r^{(sf)}\right)-\frac{R_s}{\sigma L_s}\left(\underline{\lambda}_s^{(sf)}-\hat{\underline{\lambda}}_s^{(sf)}\right)-\mathrm{j}\omega_{sf}\left(\underline{\lambda}_s^{(sf)}-\hat{\underline{\lambda}}_s^{(sf)}\right)-\underline{k}_1\underline{\mu}^{(sf)}, \tag{10}$$

$$\frac{\mathrm{d}}{\mathrm{d}t}\left(\underline{\lambda}_r^{(rf)}-\hat{\underline{\lambda}}_r^{(rf)}\right)=\frac{R_rL_m}{\sigma L_rL_s}\left(\underline{\lambda}_s^{(sf)}-\hat{\underline{\lambda}}_s^{(sf)}\right)-\frac{R_r}{\sigma L_r}\left(\underline{\lambda}_r^{(rf)}-\hat{\underline{\lambda}}_r^{(rf)}\right)-\mathrm{j}\left(\omega_{rf}-\omega_r\right)\left(\underline{\lambda}_r^{(rf)}-\hat{\underline{\lambda}}_r^{(rf)}\right)-\underline{k}_2\underline{\mu}^{(rf)}. \tag{11}$$

Both of candidate Lyapunov's function and attraction condition, used to reflect the characteristic of the FSMO, are given by

$$V(\underline{s})=\frac{1}{2}\left(\underline{i}_s^{(s)}-\hat{\underline{i}}_s^{(s)}\right)^T\left(\underline{i}_s^{(s)}-\hat{\underline{i}}_s^{(s)}\right). \tag{12}$$

It is noticed that, when the system reaches the sliding mode surface, the inequality condition will be

$$\underline{k}_1\frac{L_r}{L_m}-\underline{k}_2\rangle \mathrm{MAX}\left|-C_1+C_2\right| \tag{13}$$

with C_1 and C_2 are two coefficients given by

$$C_1=\frac{R_s}{\sigma L_s}\left(\frac{L_r}{L_m}-\frac{L_m}{L_r}\right)\hat{\underline{\lambda}}_s,$$

$$C_2=\mathrm{j}\omega_\mathrm{r}+\frac{R_r}{\sigma L_r}\left(\frac{L_r}{L_s}-\frac{L_m}{L_r}\right)\hat{\underline{\lambda}}_r.$$

In a first step, the no-load operating-mode with low rotating speed (*frequency* = ±3 Hz) is adopted to verify the feasibility of the proposed FSMO. Moreover, two other sliding surfaces are implemented to compare the performances of the FSMO algorithm. As illustrated in Figs. (3.a), (4.a) and (5.a), experimental results of the estimated stator current versus the actual current are presented. In Figs (3.b), (4.b) and (5.b), the stator-current error between the estimated and the actual values are shown when signum function, saturation function, and FLC are used respectively. From the above figures, the accuracy of the proposed algorithm which is based on a Tkagi-Sugeno fuzzy logic controller is better than the accuracy when we use the saturation function. Moreover, if we compare the accuracy of the proposed algorithm and the signum function, we can't see a huge difference despite the use of less switching in FLC approach, which gives more stability to the system.

The *d* and *q* components of the stator flux are shown in Fig. 6. Where, we can see the good estimation of the proposed observer even at low speeds operation mode, which is representing a real challenge for all induction motor-based, drives. It can be noted that the flux estimation is based on the measured currents and the motor speed is calculated from the flux estimation. Thus, we can compare the measured speed with their estimated value to conclude that our flux estimation is true.

In a second step, to prove the merits of the proposed FSMO, the whole algorithm is susceptible to several tests, as well as speed reversal and transition tests. In Fig. 7, the transition from the rotor speed of +450 rpm/min to 150 rpm/min is illustrated. In the same figure, the error between the estimated speed and the real speed is presented. Moreover, In Fig. 8 for speed reversal operation, we can see that the estimated speed value follows well the actual value; this can prove the correct estimation of the stator current since the rotor speed estimation is heavily based on the rotor flux estimated value.

From the above figures, it can be concluded that the proposed algorithm is well suitable for these types of drives since it gives good accuracy and offers high dynamics

4. CONCLUSIONS

In this paper, an accurate IM-current estimation algorithm based FSMO is presented. Using a DS1104 controller board performs an experimental validation of the proposed scheme. The proposed technique is fully speed-sensorless based on Takagi-Sugeno fuzzy controller and Lyapunov's theory. Moreover, a volt per hertz (*v/f*) control strategy is used to generate the switching signals of the voltage source inverter VSI. Thus, an accurate and inherently speed-sensorless observer has been performed in a dual-reference frame based on the stator and rotor flux models and a Takagi-Sugeno fuzzy controller. The stability of the proposed scheme has been demonstrated using Lyapunov's concept. The experimental results are shown and discussed for different operating modes.

Received on 29 April 2021.

APPENDIX

Data of the used Induction Motor

Rated power	3 kW
Voltage	400 V
Current	6.6 A
Rated speed	1420 rpm
Number of pole-pairs	2
R_s	1.98 Ω
R_r	1.78 Ω
L_s	0.2406 H
L_r	0.2406 H
L_m	0.2303 H
T_r	L_r / R_r
σ	$(1-(L^2_m/L_s L_r))$

REFERENCES

1. A. Ahriche, M. Kidouche, S. Mekhilef, *Robust sensorless sliding mode flux observer for DTC-SVM-based drive with inverter nonlinearity compensation*, J. of Power Electronics, **14**, *1*, pp. 125–134 (2014).
2. L. Zhao, B. Zhang, H. Yang, Y. Wang, *Finite-time tracking control for pneumatic servo system via extended state observer*, IET Control Theory Appl, **11**, pp.2808-2816 (2017).
3. H. Gue, H. Chen, T. Song, *Tire-road forces estimation based on sliding mode observer*, IEEE international conference on mechatronics and automation, Changchun, China, August. 9–12 (2009).
4. V. Utkin, J. Guldner, J. Shi, *Sliding mode control in electro-mechanical systems*, CRC Press, Taylor & Francis Group (2009).
5. L. Khelouat, A. Ahriche, S. Mekhilef, *State feedback control for stabilization of PMSM-based servo-drive with parametric uncertainty using interval analysis,* International Transactions on Electrical Energy Systems **31**, *11* (2021).
6. C. Lascu, I. Boldea, F. Blaabjerg, *A class of speed-sensorless sliding-mode observers for high-performance induction motor drives*, IEEE Trans. Ind. Electron, **56**, pp.3394–3403 (2009).
7. Z. Xu, M. F. Rahman, *Comparison of a sliding observer and a Kalman filter for direct-torque-controlled IPM synchronous motor drives*, IEEE Trans. Ind. Electron, **59**, pp. 4179–4188 (2012).
8. Z. Qiao, T. Shi, Y. Wang, Y. Yan, C. Xia, X. He, *New sliding-mode observer for position sensorless control of permanent magnet synchronous motor*, *IEEE Trans. Ind. Electron*, **60**, pp.710–719 (2013).
9. H. Kim, J. Son, J. Lee, *A high-speed sliding-mode observer for the sensorless speed control of a PMSM*, IEEE Trans. Ind. Electron, **58**, pp. 4069–4077 (2011).
10. M.L. Corradini, G. Ippoliti, S. Longhi, G. Orlando, *A quasi-sliding mode approach for robust control and speed estimation of PM synchronous motors*, IEEE Trans. Ind. Electron., **59**, pp.1096–1104 (2012).
11. V.Q. Leu, H.H. Choi, J.W. Jung, *fuzzy sliding mode speed controller for PM synchronous motors with a load torque observer*, IEEE Trans. Ind. Electron., **27**, pp.1530–1539 (2012).
12. R. Miranda, I. Chairez, J. Moreno, *Observer design for a class of parabolic PDE via sliding modes and backstepping*, 11th international workshop on variable structure systems, Mexico City, Mexico, June. 26–28 (2010).
13. Deia, M. Kidouche, A. Ahriche, *Fully decentralized fuzzy sliding mode control with chattering elimination for a quadrotor attitude*, IEEE International Conference on Electrical Engineering, Boumerdes, Algeria, December 13–15 (2015).
14. A. Ahriche, M. Kidouche, A. Idir, *Combining sliding mode and second Lyapunov function for flux estimation,* Rev. Roum. Sci. Techn. – Electrotechn. et Energ., **61**, 2, pp. 106-110 (2016).
15. B. Bouchiba, A. Hazzab, and H. Glaoui, *Multiple-Input multiple-output fuzzy sliding mode controller for multi-motors system,* Rev. Roum. Sci. Techn.–Électrotechn. et Énerg, **57**, *2*, pp. 202-211 (2012).
16. L. Youb and A. Crăciunescu, *Commande directe de couple et commande vectorielle de la machine asynchrone,* Rev. Roum. Sci. Techn. – Électrotechn. et Énerg., **53**, *1*, pp. 87-98, (2008).
17. P. Vas, *Sensorless Vector and Direct Torque Control*. Oxford, U.K Oxford Univ. Press (1998).
18. O. Chee-mun, *Dynamic simulation of electric machinery using MATLAB/SIMULINK*, Prentice Hall PTR, Chap. 6, 1998.